

NUMERICAL SIMULATION AND ANALYSIS OF CHAOS IN THE TORSION PENDULUM SYSTEM

Alex Angus

The torsion pendulum system is analyzed with different parameters resulting in chaotic and non-chaotic behavior. Numerical integration methods are used to temporally discretize the ordinary differential equations describing the Torsion Pendulum system that have no known analytical solutions. The numerically obtained solutions are studied in comparison to the physical system under Fourier power spectra, Poincaré plots, and Lyapunov exponents.

Keywords: Torsion Pendulum, Chaos, Numerical Integration, Fourier, Poincaré, Lyapunov Exponents

I. INTRODUCTION

A chaotic system is characterized by an extreme dependence on initial conditions. Similar trajectories of this system at first appear to exhibit the same dynamics, but over time diverge into seemingly random behavior. Chaotic systems are, however, deterministic in nature. Thus, they are often described by nonlinear differential equations, many of which do not have analytical solutions and require numerical methods to approximate solutions.

Characteristics of relatively simple nonlinear chaotic systems, like the Torsion Pendulum, are generalizable to larger real world systems. Additionally, the description of a chaotic system provides another avenue to express uncertainty [1]. Instead of a probabilistic concepts of uncertainty, we can express models of chaos in terms of their temporal instability. The accurate prediction duration of a chaotic model is limited, as the prediction error increases exponentially with time.

The Torsion Pendulum System

The Torsion Pendulum system is illustrated in Figure 1 and is comprised of a circular disk with moment of inertia J connected to a torsion spring with torsion constant D . The system exhibits behavior that is an angular analogue to linear simple harmonic motion¹. We measure the angular displacement θ of the disk from equilibrium with a Pasco angle meter. The system can be driven with an external drive motor that is attached to the torsion spring by a drive arm. To determine the frequency of the drive, a drive flag is connected to the drive arm. The drive flag, which moves in phase with the drive arm, passes through a Pasco laser sensor (frequency meter) that produces a signal indicative of

the drive frequency. To produce chaotic behavior with respect to the angular displacement of the disk, we break the symmetry of the disks moment of inertia by attaching weights m_1 and m_2 at the radius and at angles θ_1 and θ_2 from the equilibrium angle θ_0 of the disk. The addition of these weights produces a variable torque on the system depending on the displacement angle θ , and can be seen in Figures 2 and 3.

The naturally damped, undriven, and non-weighted behavior of the system is described by

$$J\ddot{\theta} + r\dot{\theta} + D\theta = 0 \quad (1)$$

where r is the damping torque and $\ddot{\theta}$ and $\dot{\theta}$ are the first and second time derivatives of the angular displacement. The damped, driven, and non-weighted behavior is described by [2]

$$J\ddot{\theta} + r\dot{\theta} + D\theta = \tau_d \sin(2\pi\omega_d t) \quad (2)$$

where τ_d is the amplitude of the drive torque and ω_d is the drive frequency. Alternatively, since measuring τ_d is logistically difficult, we can express the behavior of the damped driven system by incorporating the driving into the displacement term as

$$J\ddot{\theta} + r\dot{\theta} + D[\theta + \theta_d \sin(2\pi\omega_d t)] = 0 \quad (3)$$

where θ_d is the angular drive amplitude. Finally, chaotic behavior of the torsion pendulum system is given by

$$J\ddot{\theta} + r\dot{\theta} + D[\theta + \theta_d \sin(2\pi\omega_d t)] - \tau_1 - \tau_2 = 0 \quad (4)$$

where τ_1 and τ_2 are

$$\tau_1 = m_1 g r \sin(\theta + \theta_1) \quad (5)$$

$$\tau_2 = m_2 g r \sin(\theta - \theta_2) \quad (6)$$

¹ A video of the Torsion Pendulum motion can be found [here](#).

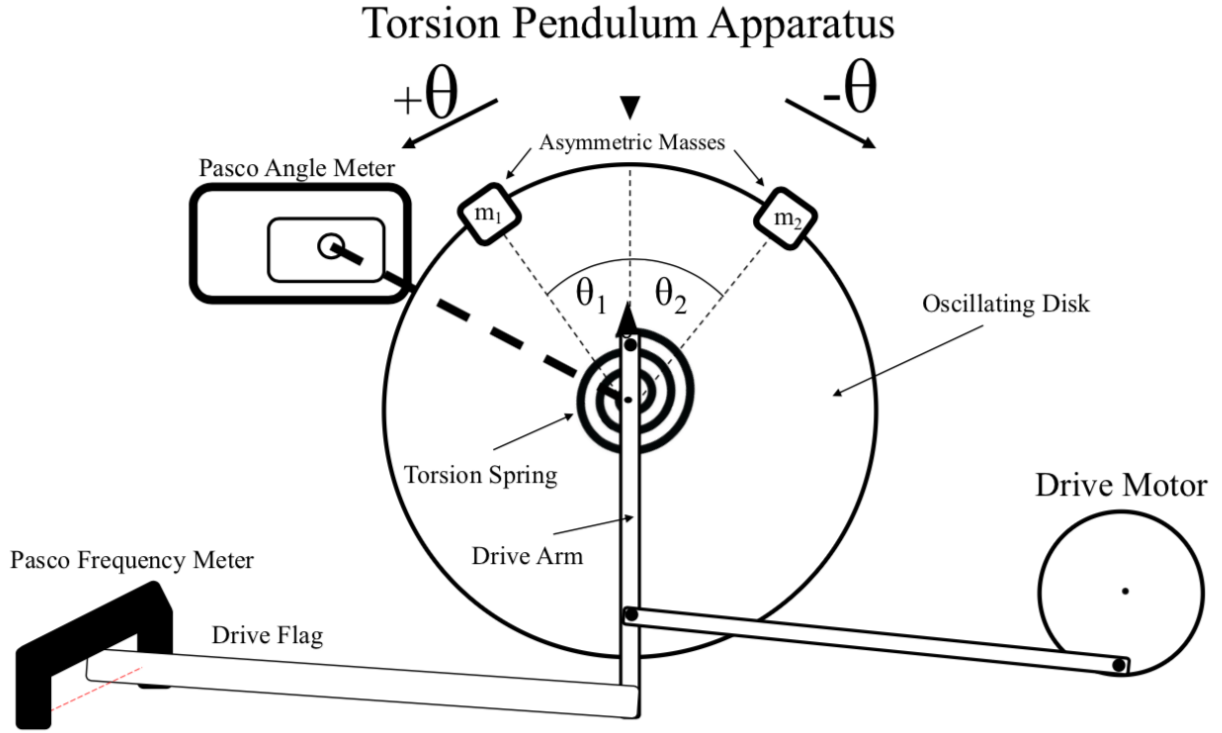


Figure 1: Schematic Diagram of the Torsion Pendulum System. Angular displacement of the Oscillating Disk in θ is measured by the Pasco Angle Meter. Excitement from the Drive Motor is added to the system via the Drive Arm, and its frequency is measured with the Drive Flag and the Pasco Frequency Meter. To disrupt the symmetry of the disk's moment of inertia, we attach the Asymmetric Masses m_1 and m_2 at θ_1 and θ_2 .

Torsion Pendulum Torques

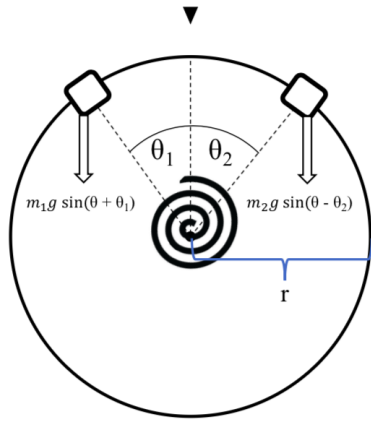


Figure 2: The Torsion Pendulum with masses attached, The forces exerted on the disk by the masses are shown as arrows. These forces are proportional to the torques exerted on the disk in the θ direction.

which correspond to the torques from m_1 and m_2 . The chaotic behavior described by (4) can be partially explained as a result of this system's potential energy function. The potential energy U of (4) is derived by summing the torques τ_1 , τ_2 , and $D\theta$ and integrating

Torsion Pendulum Torques

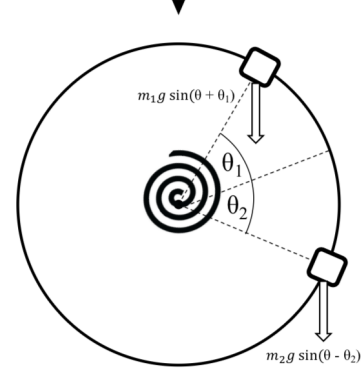


Figure 3: Forces acting on the Torsion Pendulum. As the displacement from equilibrium $\Delta\theta$ increases, the torques from the additional masses cause the disk to move away from the equilibrium position θ_0 at an increasing rate until the motion is again dominated by the torque of the torsion spring $D\theta$.

with respect to θ . The result is

$$U(\theta) = \frac{1}{2}(D\theta^2 - 2gr(m_1\cos(\theta - \theta_1) + m_2\cos(\theta + \theta_2))). \quad (7)$$

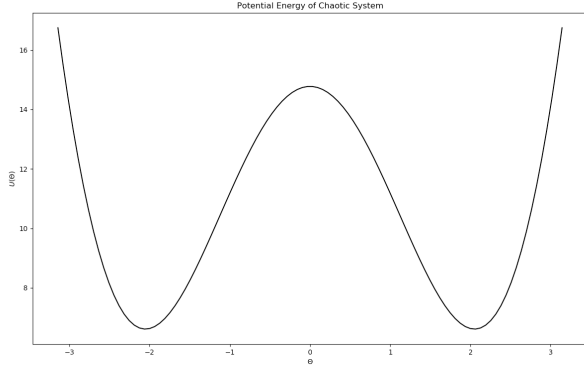


Figure 4: Double well potential energy as a function of angular displacement in the chaotic torsion pendulum system (7).

This potential energy function has a double well shape (Figure 4) that is characteristic of many chaotic mechanical systems such as those in [3].

II. SIMULATION OF TORSION PENDULUM DYNAMICS

Numerical Integration

Apart from (1), the differential equations that describe the Torsion Pendulum system do not have analytical solutions. Therefore we must use numerical integration to approximate solutions to these equations if we are to predict and simulate the system's behavior. To accomplish this we use the Python `scipy.integrate` module. As these equations are second order differential equations, we must first separate them into two first order equations and solve them as a system of equations. Once they are separated, we use the `odeint` package to iteratively step through time from the initial conditions of the system for approximate solutions at each time.

Parameter Tuning with Damped Undriven and Damped Driven Motion

First, we analyze the system in the simplest case: undriven without weights. To tune the damping constant r and the torsion spring constant D ², we fit the damped undriven integration model based on (1) to real recorded data of an undriven oscillation. This fit can be seen in Figure 5, and, when compared to a different set of real undriven data, the numerical integration model has a mean squared error on the order of 10^{-3} . A similar method is used for tuning the drive amplitude parameter θ_d . This fit can be seen in Figure 6.

² The moment of inertia of the disk J was determined by weighing the disk and approximating it as a two dimensional uniform disk.

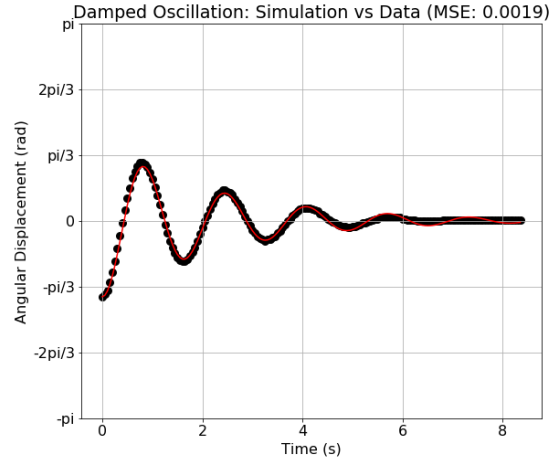


Figure 5: Damped Undriven Motion of the Torsion Pendulum. The prediction is plotted in red on top of the real data in black. The numerical integration model achieves a mean squared error on the order of 10^{-3} in comparison to measured data.

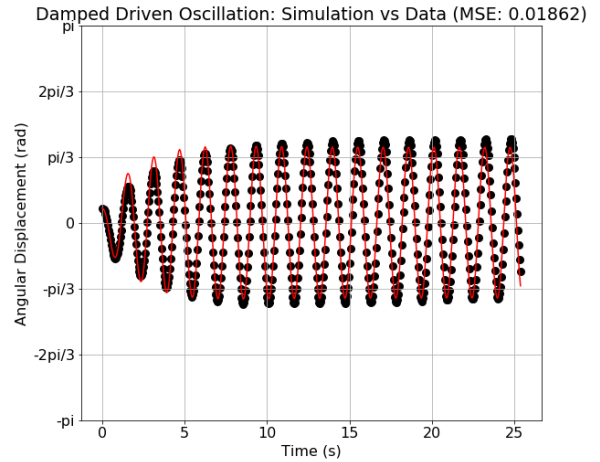


Figure 6: Damped Driven Motion of the Torsion Pendulum. The prediction is plotted in red on top of the real data in black. The numerical integration model achieves a mean squared error on the order of 10^{-2} in comparison to measured data.

Simulating Chaos

To simulate chaos, we incorporate the asymmetric weight terms into our damped driven model to give the potential energy function its characteristic double well shape. We assume that any mass differences or angle placement differences in the real system are negligible such that in our numerical model $m_1 = m_2 = m$ and $|\theta_1| = |\theta_2| = \theta_m$. Figure 8 shows measured angle-time data of the physical Torsion Pendulum in its chaotic configuration, and Figure 7 shows a phase diagram of

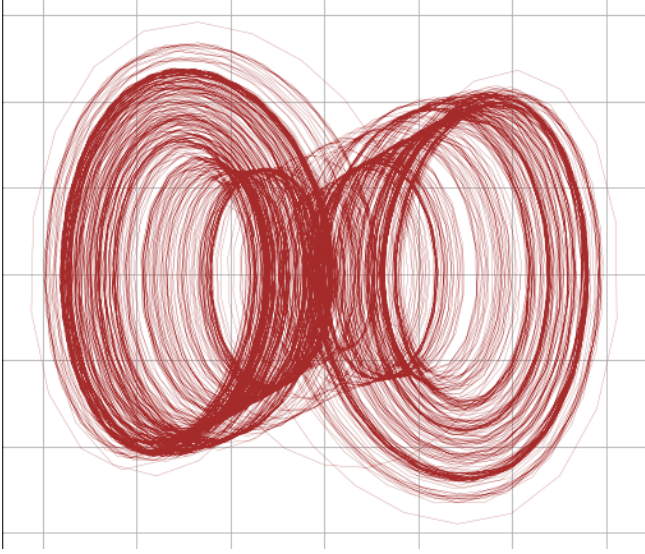


Figure 7: Qualitative Phase Plot of Torsion Pendulum Chaotic Behavior. Vertical axis is $\dot{\theta}(t)$ and horizontal axis is $\theta(t)$.

the same. The displacement over time varies at non-uniform, unpredictable intervals in both the physical system and the simulated system. An advantage of the simulated system, however, is that it can calculate the behavior for an arbitrarily long interval of time without actually waiting that time for the results. Therefore, we are able to see the behavior much longer into the future in the simulation in comparison to the real physical system. We also see that both the simulation and physical systems are extremely sensitive to changes in the initial conditions. This is evident in Figure 9, as it shows the behavior of two instances of the chaotic simulation over 5000 seconds with a 10^{-3} difference in initial displacement.³ The long term behavior of this system is unpredictable, and it is clear that differences in initial conditions as small as 10^{-3} have a significant impact after the first couple seconds of the oscillation. To illustrate the divergence in behavior of systems with extremely similar, but not identical initial conditions, we examine Figures 10 and 11. Figure 10 shows divergence with $\Delta\theta_0 = 10^{-3}$ and Figure 11 shows divergence with $\Delta\theta_0 = 10^{-4}$. In both cases behavior coherence is observed for a period of time, then the different instances diverge into seemingly random behavior. With the given initial conditions, this coherence period lasts for approximately 8 seconds in the $\Delta\theta_0 = 10^{-3}$ case, and 24 seconds in the $\Delta\theta_0 = 10^{-4}$ case. From this example it is easy to see how prediction error increases exponentially with time in chaotic

³ The initial velocity of both instances is $\dot{\theta}_0 = 0$.

systems⁴. If prediction error scaled linearly with initial condition precision, then we would expect the coherence period of the $\Delta\theta_0 = 10^{-4}$ case to be about 80 seconds, but this is clearly not the case. An animation of this phenomenon can be found [here](#).

III. ANALYSIS OF CHAOS

Fourier Analysis

Fourier techniques are used to decompose a signal into its fundamental components. Any signal (function) can be represented as a superposition of oscillations, each with a different frequency, where some frequencies contribute more than others. The discrete Fourier transform F_k of f is given by (8) [5].

$$F_k = \sum_{n=0}^{N-1} f_n \cdot e^{-\frac{i2\pi}{N}nk} \quad (8)$$

For a predictable, non-chaotic signal we expect the Fourier decomposition to reveal a finite and relatively small quantity of frequencies that contribute to the overall behavior of the system in question. The opposite is true for a chaotic system. If the behavior is indeed chaotic, then we expect a large number of contributing frequencies. This is evident in the Fourier transform of a simulated angle-time signal shown Figure 12. The Fourier transform reveals a large number of fundamental frequencies present in the angular displacement. This suggests that the behavior is chaotic. Additionally, we see a large spike at 0.6 Hz, which is, in this case, the frequency of the drive f_d .

Poincaré Plots

Poincaré plots are used to distinguish randomness from chaos. They are a higher dimensional representation of data that makes it easier to determine periodicity, or the lack thereof. In relation to the Torsion Pendulum system, we sample the angular velocity $\dot{\theta}$ and angular displacement θ of the system at uniform intervals. This can be seen in Figures 13 and 14. These Poincaré plots reveal a hidden structure that is invisible in a one dimensional analysis. It suggests this motion is not random, and instead that it is quasiperiodic, or exhibiting a frequency that changes over time. We can see visually

⁴ Because of this (and the sheer number of system parameters), it is extremely difficult to get agreement between simulated and measured chaotic systems. For a strong agreement, more robust computing methods are needed such as those discussed in [4]. Additionally, in our specific apparatus, the drive mechanism did not produce a uniform sinusoidal drive, so comparison between simulated and measured chaos is impossible.

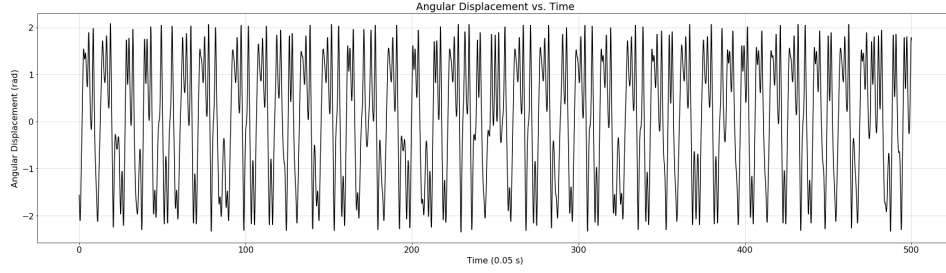
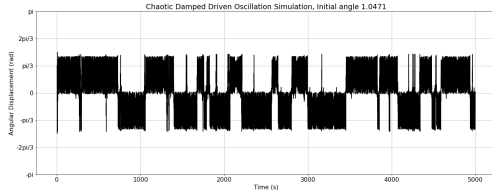
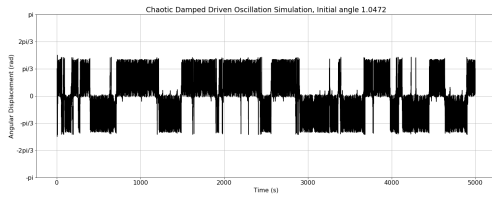


Figure 8: Chaotic behavior of the physical Torsion Pendulum. The displacement over time is unpredictable, yet deterministic. The Maximum Lyapunov Exponent of this run was calculated with the Rosenstein algorithm to be 0.0252, which indicates that this system is indeed chaotic.



(a) Simulation of the Chaotic Torsion Pendulum with $\theta_0 = 1.0471$ and $\dot{\theta}_0 = 0$.



(b) Simulation of the Chaotic Torsion Pendulum with $\theta_0 = 1.0472$ and $\dot{\theta}_0 = 0$.

Figure 9: Two instances of the Chaotic Torsion Pendulum simulation with $\Delta\theta_0 = 10^{-3}$. It is impossible to predict the behavior of this system in a large enough time interval.

(and have confirmed numerically) that two points on these graphs cannot overlap⁵. If they were to overlap, then the two systems would converge and evolve identically from that point because the system is deterministic. In most configurations of the Torsion Pendulum this does not happen, but for some it does. Specific initial conditions result in this converging behavior, and this can be seen in Figure 15. In Figure 15 we see that the motion starts in a chaotic manner, but converges to a finite number of states after ample time. The reason for this convergence is not immediately clear, but is certainly a result of specific combinations of system

⁵ This is of course within the limits in accuracy of floating point numbers on the computer.

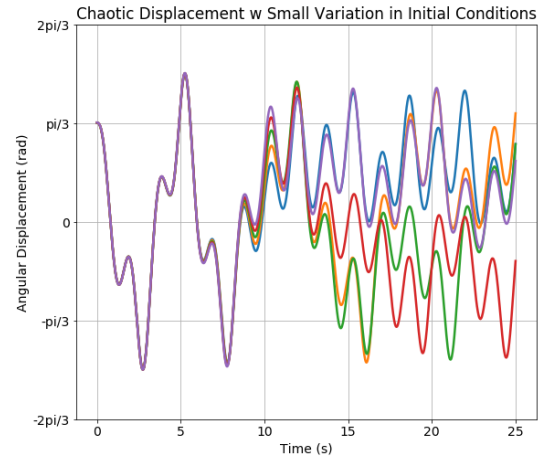


Figure 10: Comparison of long term behavior with small changes in initial conditions. This example shows instances of the simulated Torsion Pendulum with $\Delta\theta_0 = 10^{-3}$ difference in initial displacement. Initial angular velocity $\dot{\theta}_0 = 0$ for all instances.

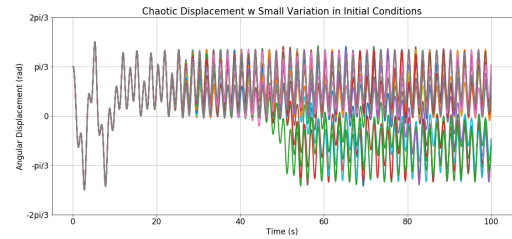


Figure 11: Comparison of long term behavior with small changes in initial conditions. This example shows instances of the simulated Torsion Pendulum with $\Delta\theta_0 = 10^{-4}$ difference in initial displacement. Initial angular velocity $\dot{\theta}_0 = 0$ for all instances.

parameters and initial conditions. A distribution of chaotic and periodic behavior as a function of initial conditions is seen in Figure 16.

Fourier Spectrum of Chaotic Displacement Signal. $\theta_0 = 0.7854$

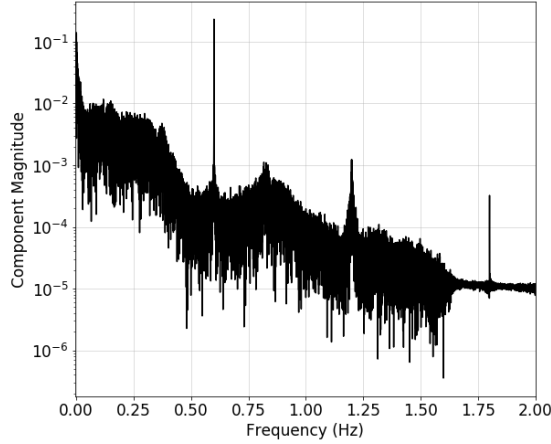


Figure 12: Fourier Transfer of Simulated Chaotic Displacement Signal with $\theta_0 = 0.7854$. The chaotic behavior is the result of a large number of contributing fundamental frequencies. The drive frequency of the system exhibits a large spike at $f = 0.6$.

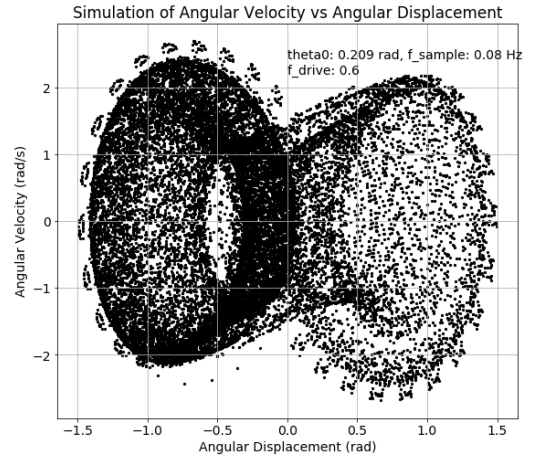


Figure 14: Poincaré plot of the chaotic Torsion Pendulum Simulation with $\theta_0 = 0.209$ rad, $f_d = 0.6$ Hz, and $f_{sample} = 0.08$ Hz. This higher dimensional representation of the displacement and velocity data reveals a hidden structure that indicates chaos.

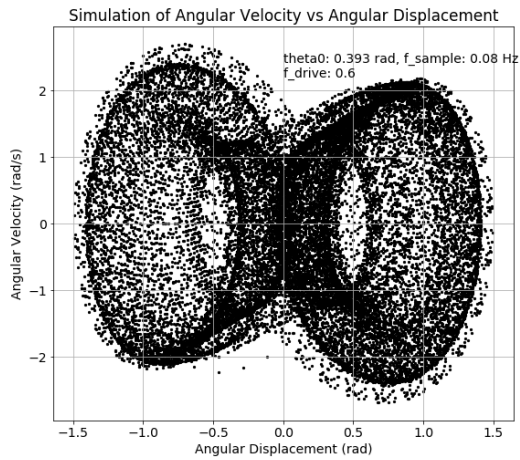


Figure 13: Poincaré plot of the chaotic Torsion Pendulum Simulation with $\theta_0 = 0.393$ rad, $f_d = 0.6$ Hz, and $f_{sample} = 0.08$ Hz. This higher dimensional representation of the displacement and velocity data reveals a hidden structure that indicates chaos.

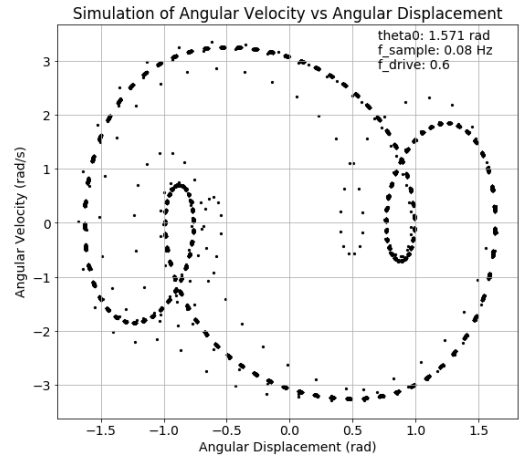


Figure 15: Poincaré plot of the chaotic Torsion Pendulum Simulation with $\theta_0 = 1.571$ rad, $f_d = 0.6$ Hz, and $f_{sample} = 0.08$ Hz. This higher dimensional representation of the displacement and velocity data reveals a periodic structure.

Lyapunov Exponents

The calculation of Lyapunov Exponents is another method of analyzing diverging systems. By definition, a Lyapunov Exponent is a value that characterizes the rate of separation of two infinitesimally similar trajectories. The Maximum Lyapunov Exponent (MLE) is the maximum divergence that these two trajectories can exhibit. Formally, we have that the MLE of the discrete

Torsion Pendulum system is [6]

$$\lambda(\theta_0) = \lim_{t \rightarrow \infty} \frac{1}{t} \sum_{i=0}^{t-1} \ln(f'(\theta_i)) \quad (9)$$

where λ is the Lyapunov Spectrum as a function of initial conditions θ_0 , and f is (4) solved for $\ddot{\theta}$ as a function of θ , $\dot{\theta}$, and f_d .

The MLE is quantity whose dimension is determined by the time interval of samples, thus it is often analyzed without regard to dimension and with a focus on sign.

Chaos with Different Initial Conditions

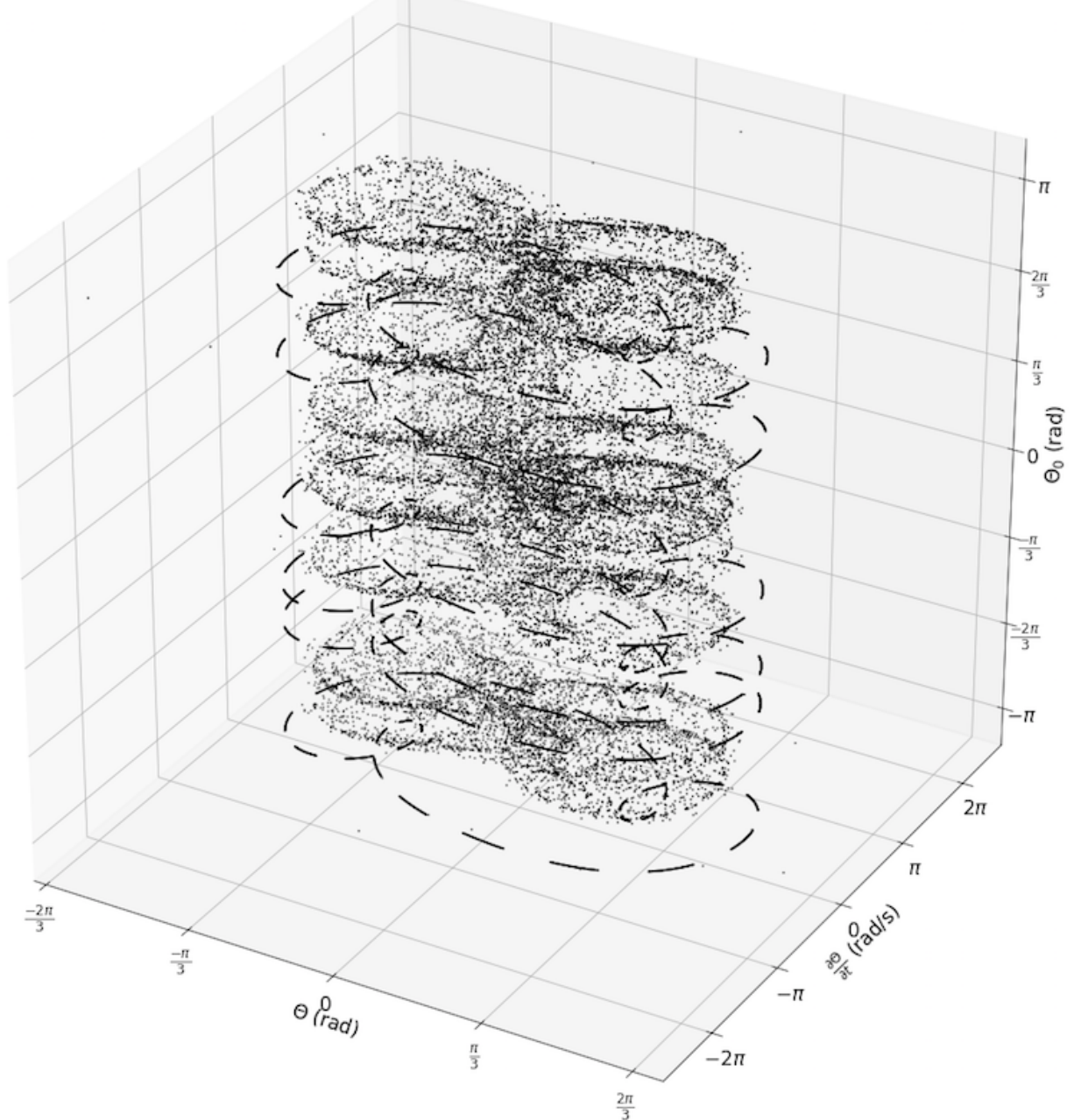


Figure 16: A Three Dimensional Poincaré plot. This plot shows that with some initial conditions the resulting behavior of the Torsion Pendulum is chaotic, and at some it is periodic.

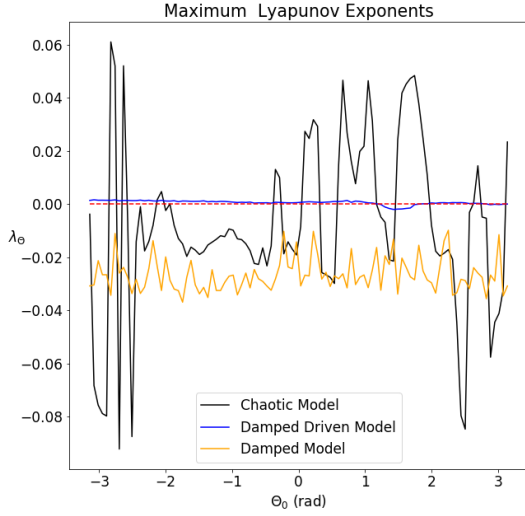


Figure 17: Plot of Maximum Lyapunov Exponent as a function of initial angular displacement. Shown are the MLE for the chaotic, damped driven, and damped undriven configurations of the Torsion Pendulum simulation. The chaotic model yields a positive MLE for certain initial displacements, confirming its chaotic nature, the damped driven model yields a MLE of approximately zero, indicating that it maintains a steady number of states no matter the initial conditions, and the undriven model demonstrates its convergence as it yields a negative MLE for all initial displacements.

Whether the MLE is positive, negative, or zero is indicative of the type of behavior in question. A positive MLE strongly suggests chaotic time series behavior, as the exponential divergence is high. A MLE of zero indicates that the system is neither diverging nor converging, but retaining a steady number of states through time, which is the characteristic of a driven oscillation. A negative MLE indicates that the number of states decreases with time, and eventually, at a large enough time, there will be no variation in trajectory⁶.

To implement MLE calculations, we use the Python **nolds** module and the **lyap-r** function. Specifically, we calculate the MLEs of the chaotic angular displacement signals using the Rosenstein algorithm described in [7]. In Figure 17 we show the MLE of the three Torsion Pendulum systems (Damped, Damped Driven, Chaotic) as a function of initial angular displacement. The results are as we expected, and they are consistent with results from the Fourier and Poincaré analyses. We observe the chaotic model to have a positive MLE at certain initial conditions, but not others, the damped driven model has a MLE consistently on the order of 10^{-4} (very close

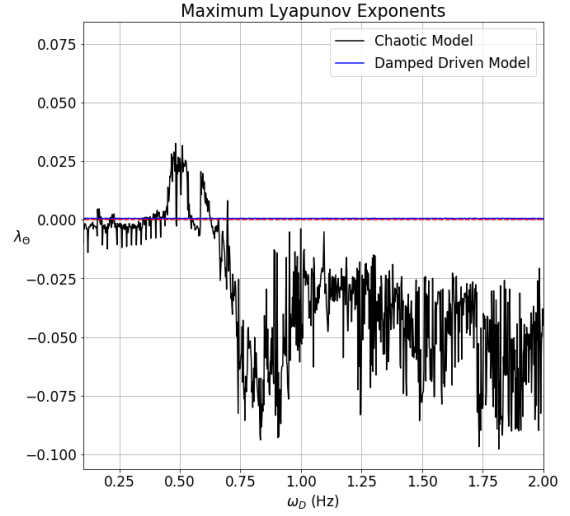


Figure 18: Plot of Maximum Lyapunov Exponent as a function of drive frequency. Shown are the MLE for the chaotic configuration and the damped driven configuration of the Torsion Pendulum simulation. The chaotic model yields a positive MLE for certain drive frequencies, confirming its chaotic nature, while the damped driven model yields a MLE of zero, indicating that it maintains a steady number of states no matter the drive frequency.

to zero), and the damped undriven model always yields a negative MLE. The MLE in angular displacement of the chaotic and damped driven models were also calculated as a function of drive frequency ω_d with similar results. In Figure 18 we see that the chaotic model again has a positive MLE for certain drive frequencies, and the damped driven model is consistently within 10^{-6} of zero.

Additionally, the MLE in angular displacement of the chaotic model was calculated as a function of both θ_0 and $\dot{\theta}_0$. These results further confirm the chaotic nature of the Torsion Pendulum simulation, and can be seen in Figures 19 and 20. These calculations reveal that specific combinations of system parameters result in highly chaotic behavior, and different specific combinations result in highly periodic behavior. It is interesting to note that these extreme combination results occur with close proximity in the initial condition space. The reason for this is not clear, and it leaves room for further work with this system.

IV. CONCLUSION

On a fundamental level, chaos indicates a limit to knowledge and to the ability to predict. It demonstrates that, without infinite precision in initial conditions,

⁶ Although it is possible to have multiple points of convergence.

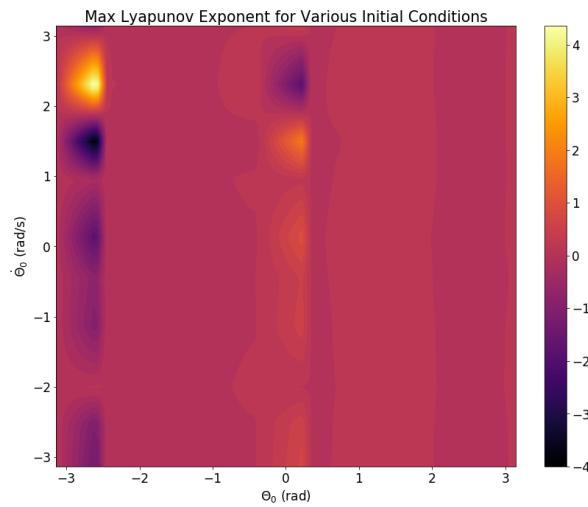


Figure 19: This two dimensional contour plot shows the Maximum Lyapunov Exponent (MLE) of the Torsion Pendulum at various initial conditions. Areas of positive MLE are chaotic in nature and exhibit a diverging behavior, whereas areas of negative MLE are periodic and exhibit converging behavior. Areas with a MLE near zero maintain a constant number of states. Note that the majority of the initial condition space results in only slightly chaotic behavior.

there will be a point or time in which our predictions are inaccurate [8]. Through analysis with Fourier decomposition, Poincaré plots, and Lyapunov Exponents, we have explored the simulated Torsion pendulum system in its numerous configurations. With Maximum Lyapunov Exponent sweeps over initial condition spaces, we have identified combinations of parameters that yield highly chaotic behavior and those that yield highly periodic behavior, though the majority of those spaces result in only slightly chaotic behavior. While its exact present predicts its exact future, the same is not true for an approximation. In summary, we have found the

Torsion Pendulum to be deterministic in nature, but nearly impossible to predict.

REFERENCES

1. Fradkov, A., Pogromsky, A. (n.d.). Nonlinear and Adaptive Control of Chaos. Handbook of Chaos Control, 129–157. doi: 10.1002/9783527622313.ch7
2. Pohl. (n.d.). Torsion Pendulum According to Prof. Pohl 1002956. Torsion Pendulum According to Prof. Pohl 1002956. 3B SCIENTIFIC PHYSICS PHYSICS.
3. Litak, G., Borowiec, M., Syta, A. (2007). Vibration of generalized double well oscillators. Zamm, 87(8-9), 590–602. doi: 10.1002/zamm.200610338
4. Fuzzy Chaotic Systems. (2006). Studies in Fuzziness and Soft Computing. doi: 10.1007/3-540-33221-9
5. Fourier Transform. (n.d.). Retrieved from <https://mathworld.wolfram.com/FourierTransform.html>
6. Cencini, M., Cecconi, F., Vulpiani, A. (2010). Chaos: from simple models to complex systems. London: World Scientific.
7. Rosenstein, M. T., Collins, J. J., Luca, C. J. D. (1993). A practical method for calculating largest Lyapunov exponents from small data sets. Physica D: Nonlinear Phenomena, 65(1-2), 117–134. doi: 10.1016/0167-2789(93)90009-p
8. Boeing, G. (2016). Visual Analysis of Nonlinear Dynamical Systems: Chaos, Fractals, Self-Similarity and the Limits of Prediction. Systems, 4(4), 37. doi: 10.3390/systems4040037

Max Lyapunov Exponent for Various Initial Conditions

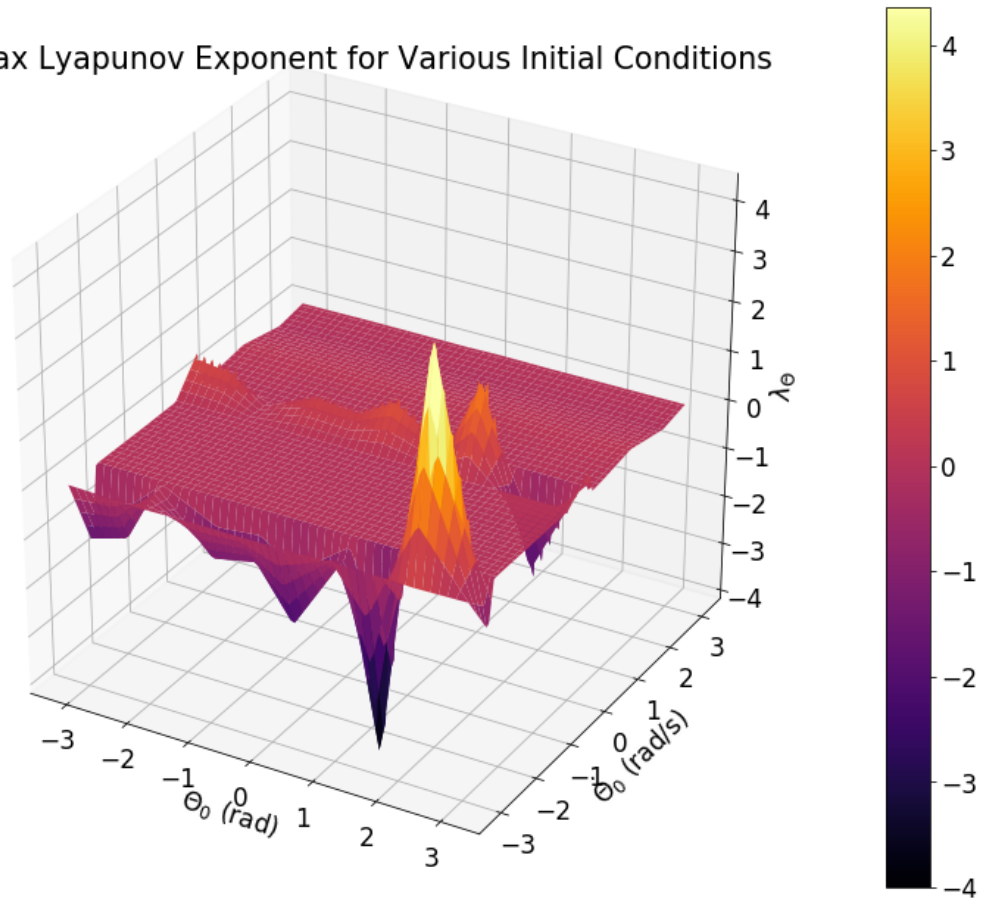


Figure 20: This three dimensional contour plot shows the Maximum Lyapunov Exponent (MLE) of the Torsion Pendulum at various initial conditions. Areas of positive MLE are chaotic in nature and exhibit a diverging behavior, whereas areas of negative MLE are periodic and exhibit converging behavior. Areas with a MLE near zero maintain a constant number of states. Note that the majority of the initial condition space results in only slightly chaotic behavior.